Mathematical
Institute

Observations of the loss landscape: impact of parameterization and architecture

Theories of Deep Learning: C6.5,
Lecture / Video 10

Prof. Jared Tanner
Mathematical Institute
University of Oxford

Oxford
Mathematics

UNIVERSITY OF OXFORD
Mathematical Institute

Consider a fully connected L layer deep net given by

$$h^{(\ell)} = W^{(\ell)} z^{(\ell)} + b^{(\ell)}, \qquad z^{(\ell+1)} = \phi(h^{\ell}), \qquad \ell = 0, \ldots, L-1,$$

for $\ell = 1, \ldots, L$ with nonlinear activation $\phi(\cdot)$ and $W^{(\ell)} \in \mathbb{R}^{n_\ell \times n_\ell}$. The trainable parameters for the DNN, $\theta := \{W^{(\ell)}, b^{(\ell)}\}_{\ell=1}^{L}$ are learned by minimizing a high dimensional, $|\theta| \sim n^2 L$, loss function such as

$$\mathcal{L}(\theta; X, Y) = (2m)^{-1} \sum_{\mu=1}^{m} \sum_{i=1}^{n_L} (H(x_\mu(i); \theta) - y_{i,\mu})^2.$$

The shape of $\mathcal{L}(\theta)$ and our knowledge about a good initial minimizer $\theta^{(0)}$ strongly influence our ability to learn the parameters θ for the DNN.

Landscape loss function: VGG9 (Li et al. 18')

One dimensional views of a loss landscape

UNIVERSITY OF OXFORD
Mathematical Institute

DNN loss $\mathcal{L}(\theta)$ between two minimizers, $\theta^s(1-\alpha)+\alpha\theta'$ trained with small and large batches; horizontal axis α in (a) and (d).

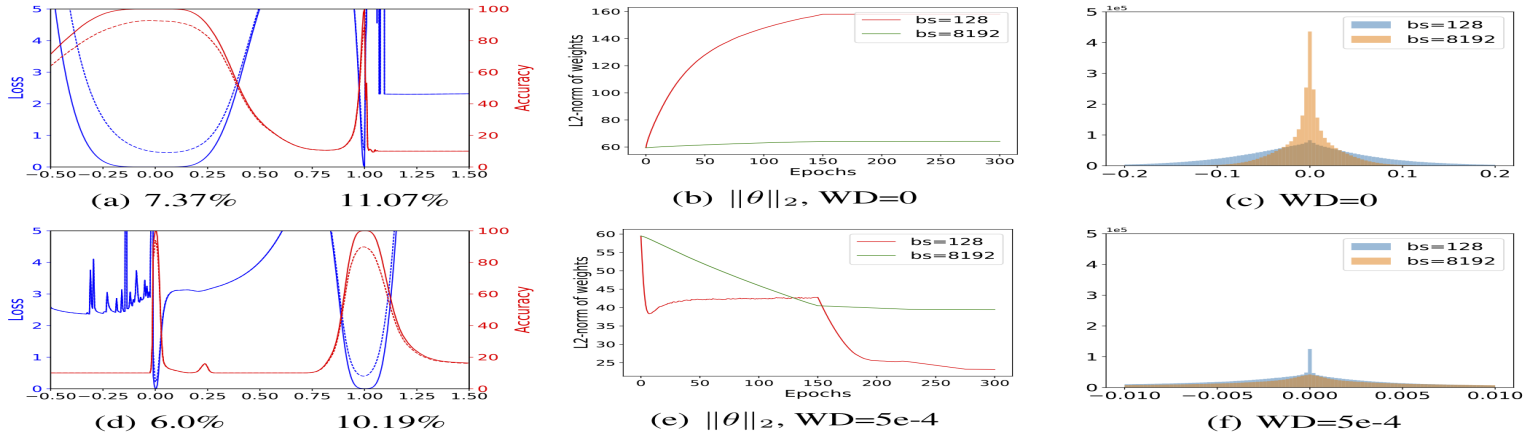

Figure 2: (a) and (d) are the 1D linear interpolation of VGG-9 solutions obtained by small-batch and large-batch training methods. The blue lines are loss values and the red lines are accuracies. The solid lines are training curves and the dashed lines are for testing. Small batch is at abscissa 0, and large batch is at abscissa 1. The corresponding test errors are shown below. (b) and (e) shows the change of weights norm $||\theta||_2$ during training. When weight decay is disabled, the weight norm grows steadily during training without constraints (c) and (f) are the weight histograms, which verify that small-batch methods produce more large weights with zero weight decay and more small weights with non-zero weight decay.

VGG9 is a CNN (Simonyan et al. 15')

`https://arxiv.org/pdf/1409.1556.pdf`

`http://papers.nips.cc/paper/7875-visualizing-the-loss-landscape-of-neural-nets.pdf`

Landscape loss function: VGG9 (Li et al. 18')

One and two dimensional landscape near SGD minima

Mathematical Institute

Impact of training rate weight decay and batch size on level curves of $\mathcal{L}(\theta^* + \alpha\delta + \beta\eta)$. Larger batch size narrows the loss function. Weight decay broadens the loss function.

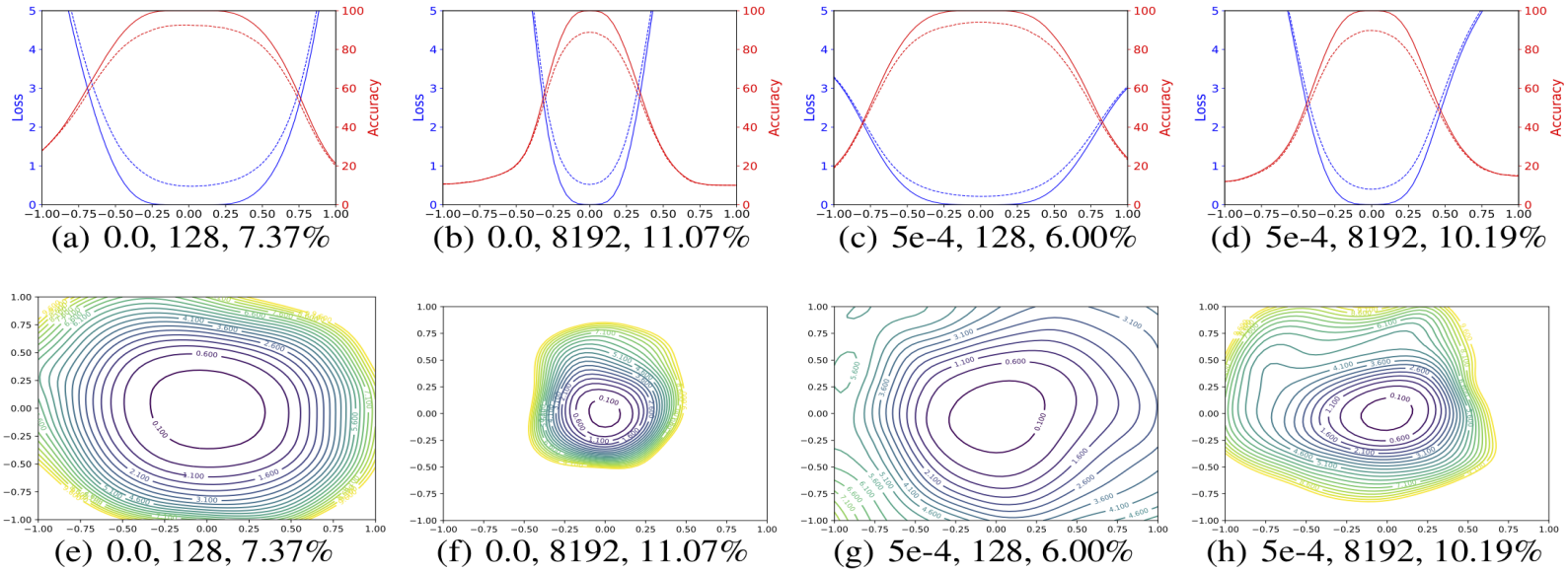

(a) 0.0, 128, 7.37% (b) 0.0, 8192, 11.07% (c) 5e-4, 128, 6.00% (d) 5e-4, 8192, 10.19%

(e) 0.0, 128, 7.37% (f) 0.0, 8192, 11.07% (g) 5e-4, 128, 6.00% (h) 5e-4, 8192, 10.19%

Figure 3: The 1D and 2D visualization of solutions obtained using SGD with different weight decay and batch size. The title of each subfigure contains the weight decay, batch size, and test error.

`http://papers.nips.cc/paper/7875-visualizing-the-loss-landscape-of-neural-nets.pdf`

Residual networks; skip connections

Residual Networks (He 15')

The skip connection building block

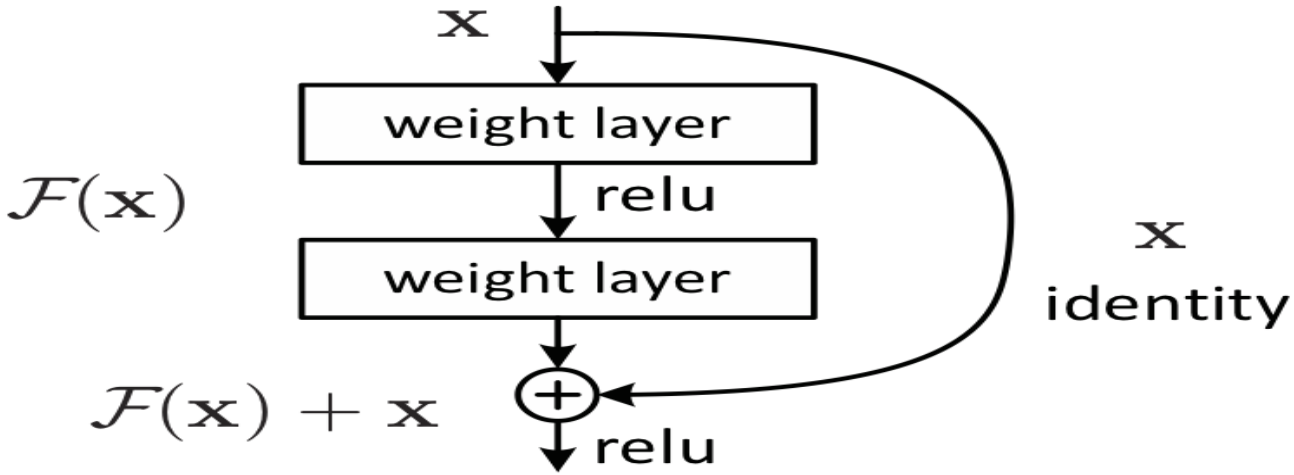

Figure 2. Residual learning: a building block.

If the block is attempting to learn a map $\mathcal{H}(x)$ the ResNet instead attempts to learn $\mathcal{F}(x) := \mathcal{H}(x) - x$ which is the residual. One can speculate this is easier to learn if $H(x)$ is approximately an identity map.

`https://arxiv.org/pdf/1512.03385.pdf`

Residual Networks (He 15')

Impact on training loss function vs without skip connections

UNIVERSITY OF OXFORD
Mathematical Institute

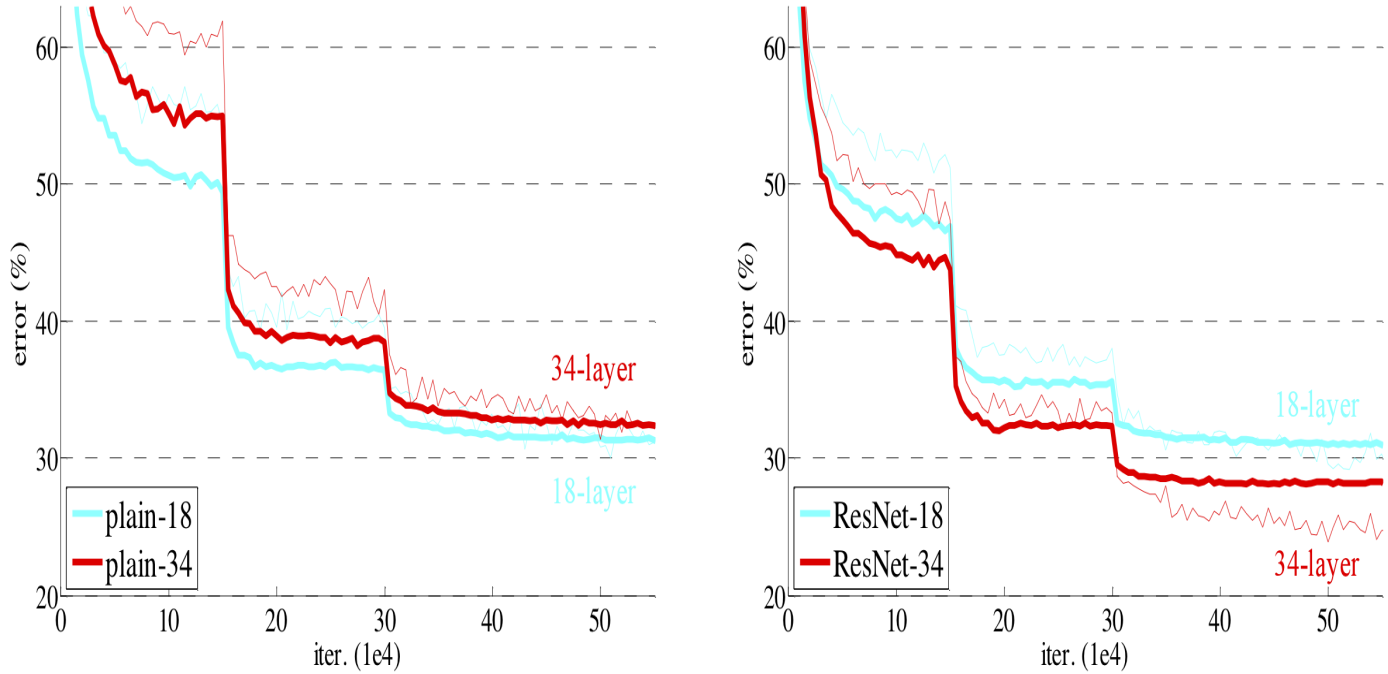

Figure 4. Training on **ImageNet**. Thin curves denote training error, and bold curves denote validation error of the center crops. Left: plain networks of 18 and 34 layers. Right: ResNets of 18 and 34 layers. In this plot, the residual networks have no extra parameter compared to their plain counterparts.

`https://arxiv.org/pdf/1512.03385.pdf`

Residual Networks (He 15')

Examples of ResNet architectures in more detail

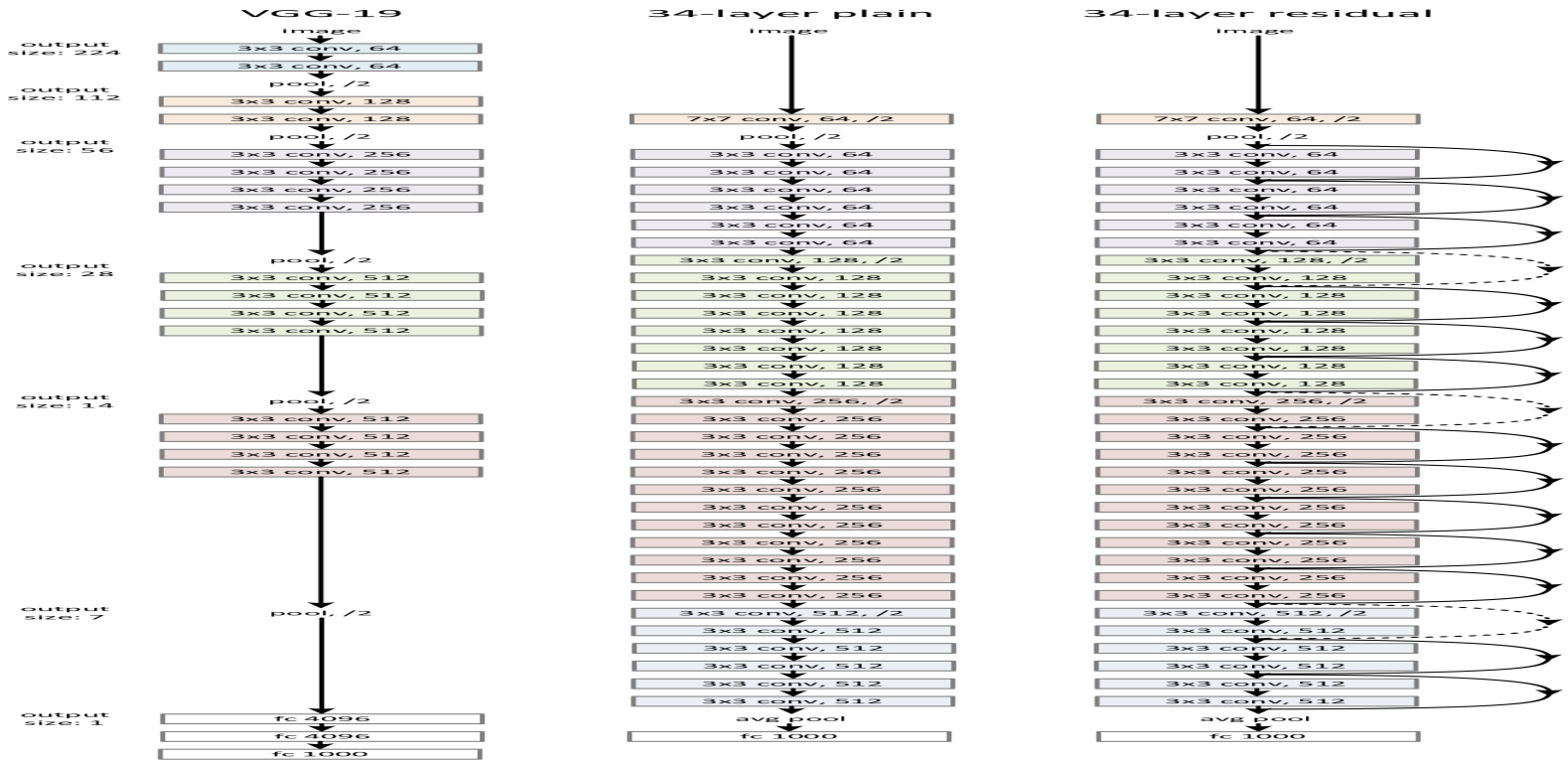

Figure 3. Example network architectures for ImageNet. **Left**: the VGG-19 model [41] (19.6 billion FLOPs) as a reference. **Middle**: a plain network with 34 parameter layers (3.6 billion FLOPs). **Right**: a residual network with 34 parameter layers (3.6 billion FLOPs). The dotted shortcuts increase dimensions. **Table 1** shows more details and other variants.

https://arxiv.org/pdf/1512.03385.pdf

Loss landscape example: ResNet skip (Li et al. 18')

Architecture influences landscape: depth and skip connections

University of Oxford
Mathematical Institute

No-short is a standard fully connected DNN, ResNet (He et al. 15') has additional connections between every second layer.

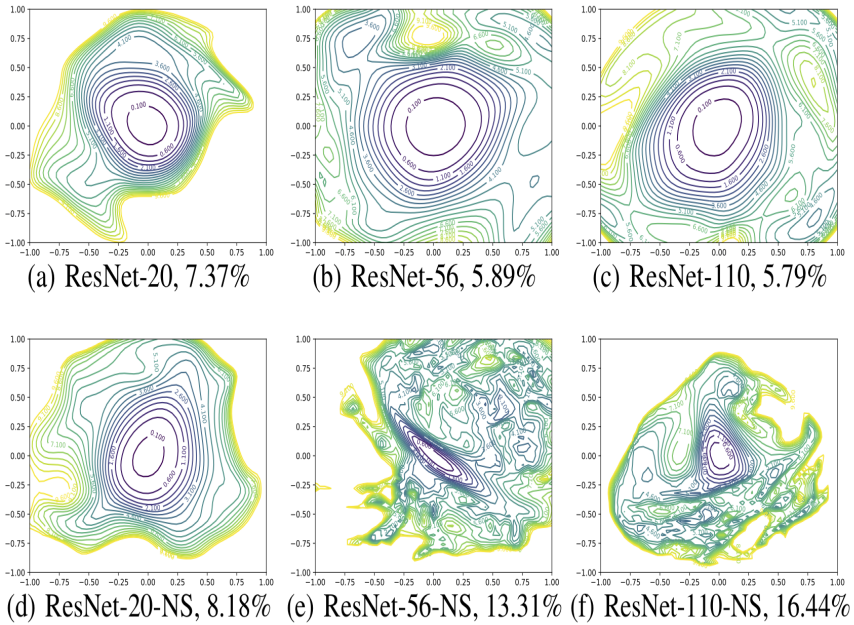

(a) ResNet-20, 7.37% (b) ResNet-56, 5.89% (c) ResNet-110, 5.79%

(d) ResNet-20-NS, 8.18% (e) ResNet-56-NS, 13.31% (f) ResNet-110-NS, 16.44%

Figure 5: 2D visualization of the loss surface of ResNet and ResNet-noshort with different depth.

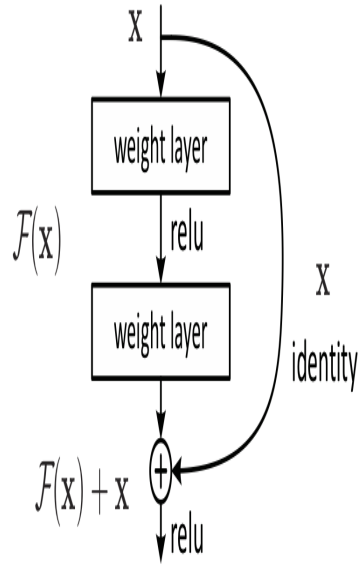

Figure 2. Residual learning: a building block.

`https://arxiv.org/pdf/1512.03385.pdf`

`http://papers.nips.cc/paper/7875-visualizing-the-loss-landscape-of-neural-nets.pdf`

Loss landscape example: ResNet-56 (Li et al. 18')

Loss landscapes are generally highly non-convex

University of Oxford
Mathematical Institute

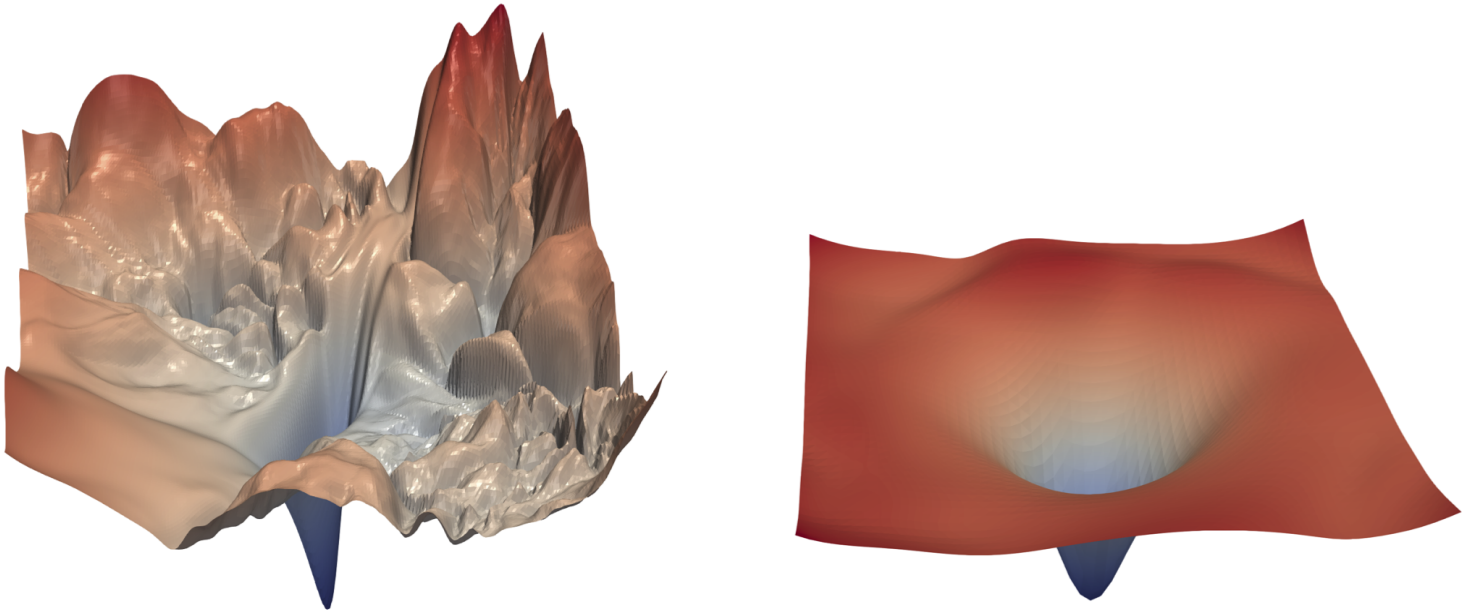

(a) without skip connections (b) with skip connections

Figure 1: The loss surfaces of ResNet-56 with/without skip connections. The proposed filter normalization scheme is used to enable comparisons of sharpness/flatness between the two figures.

`http://papers.nips.cc/paper/7875-visualizing-the-loss-landscape-of-neural-nets.pdf`

Loss landscape example: ResNet skip (Li et al. 18')

Architecture influences landscape: width

Increasing width over parameterises the net and broadens minima.

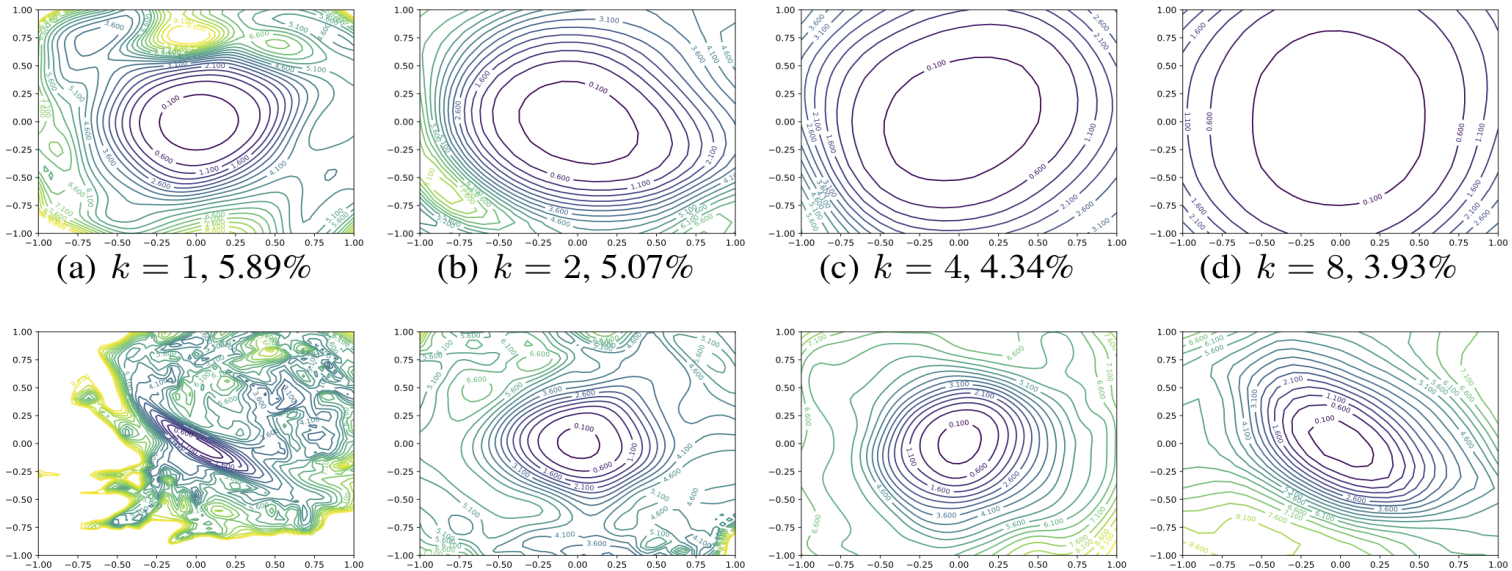

(a) $k = 1$, 5.89% (b) $k = 2$, 5.07% (c) $k = 4$, 4.34% (d) $k = 8$, 3.93%

(e) $k = 1$, 13.31% (f) $k = 2$, 10.26% (g) $k = 4$, 9.69% (h) $k = 8$, 8.70%

Figure 6: Wide-ResNet-56 on CIFAR-10 both with shortcut connections (top) and without (bottom). The label $k = 2$ means twice as many filters per layer. Test error is reported below each figure.

`http://papers.nips.cc/paper/7875-visualizing-the-loss-landscape-of-neural-nets.pdf`

Batch normalization: bulk adjusting entries

Batch normalization (Ioffe et al. 15')

Bulk normalization hyperparameters

Alternatively, bulk weight and bias normalizations, γ, and β, can be learned as part of the net parameters θ.

Input: Values of x over a mini-batch: $\mathcal{B} = \{x_{1\ldots m}\}$;
Parameters to be learned: γ, β
Output: $\{y_i = \mathrm{BN}_{\gamma,\beta}(x_i)\}$

$$\mu_{\mathcal{B}} \leftarrow \frac{1}{m}\sum_{i=1}^{m} x_i \qquad \text{// mini-batch mean}$$

$$\sigma^2_{\mathcal{B}} \leftarrow \frac{1}{m}\sum_{i=1}^{m}(x_i - \mu_{\mathcal{B}})^2 \qquad \text{// mini-batch variance}$$

$$\widehat{x}_i \leftarrow \frac{x_i - \mu_{\mathcal{B}}}{\sqrt{\sigma^2_{\mathcal{B}} + \epsilon}} \qquad \text{// normalize}$$

$$y_i \leftarrow \gamma\widehat{x}_i + \beta \equiv \mathrm{BN}_{\gamma,\beta}(x_i) \qquad \text{// scale and shift}$$

Algorithm 1: Batch Normalizing Transform, applied to activation x over a mini-batch.

https://arxiv.org/pdf/1502.03167.pdf

Batch normalization experiment (Ioffe et al. 15')

Improved initial convergence rates

Mathematical Institute

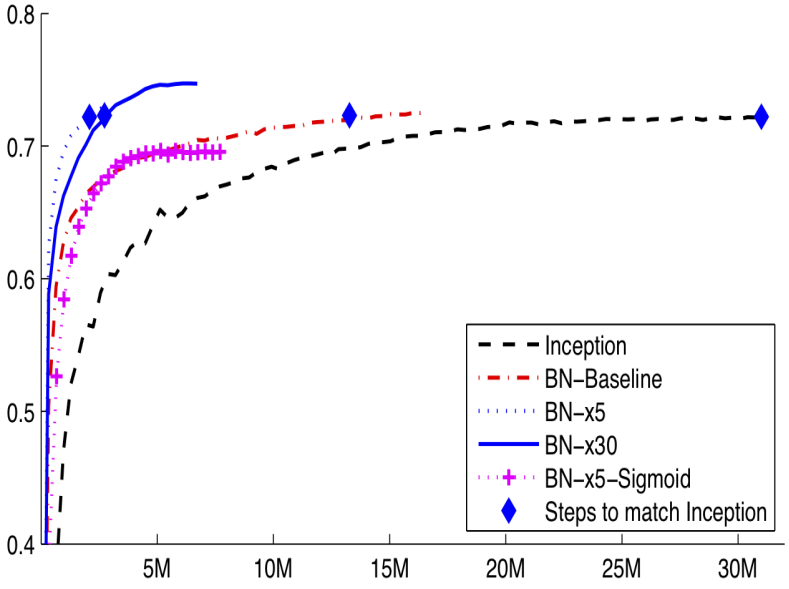

Figure 2: *Single crop validation accuracy of Inception and its batch-normalized variants, vs. the number of training steps.*

Model	Steps to 72.2%	Max accuracy
Inception	$31.0 \cdot 10^6$	72.2%
BN-Baseline	$13.3 \cdot 10^6$	72.7%
BN-x5	$2.1 \cdot 10^6$	73.0%
BN-x30	$2.7 \cdot 10^6$	74.8%
BN-x5-Sigmoid		69.8%

Figure 3: *For Inception and the batch-normalized variants, the number of training steps required to reach the maximum accuracy of Inception (72.2%), and the maximum accuracy achieved by the network.*

`https://arxiv.org/pdf/1502.03167.pdf`

Layer normalization: bulk scaling as a layer

Pre-vs-post Layer normalization (Xiong et al. 20')

Bulk normalization hyperparameters

Mathematical Institute

Layer-norm acts as batch-norm, but as the input is a matrix $X \in \mathbb{R}^{d_{ctx} \times d_{emb}}$ it can act on one input, but for each row in X. It can be applied at X fully (pre-) or just before the attention a FFN layer (post-) layer norm:

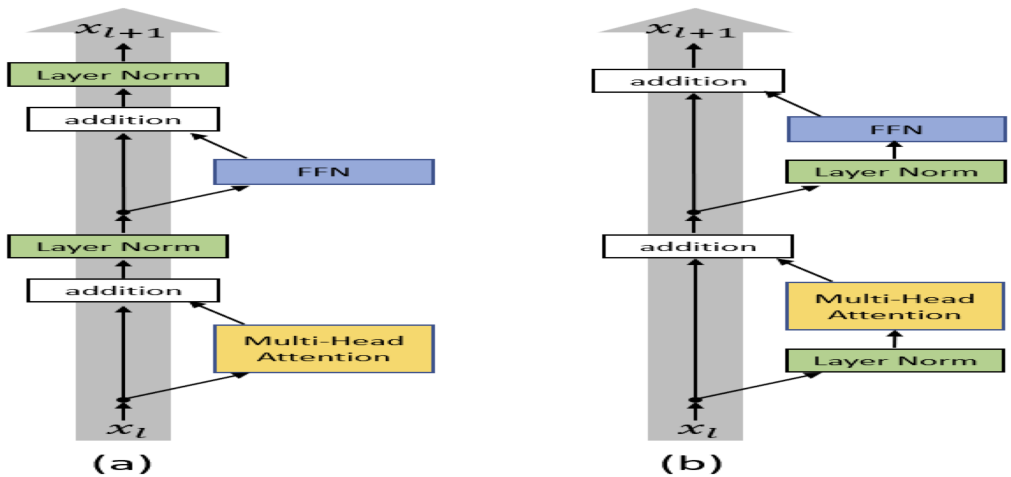

Figure 1. (a) Post-LN Transformer layer; (b) Pre-LN Transformer layer.

`https://arxiv.org/pdf/2002.04745`

Pre-vs-post Layer normalization (Xiong et al. 20')

The location of the layer-norm and gradient values

Mathematical Institute

The location of layer-norm has a substantial impact on the size of gradients per layer. This can be further impacted in "warm-up" training is done with stepsize initially starting small, then growing linearly to a maximum value.

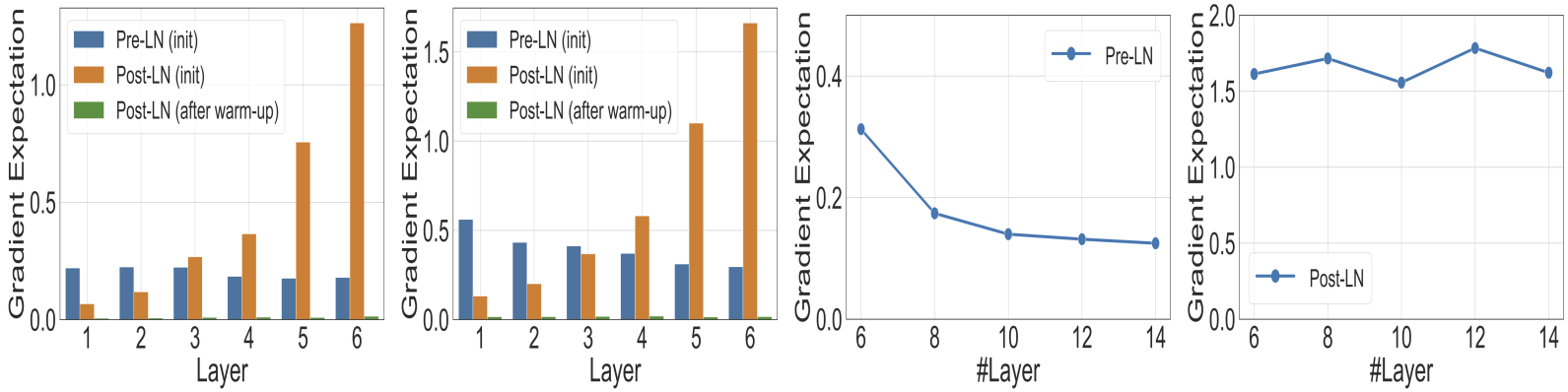

(a) W^1 in the FFN sub-layers (b) W^2 in the FFN sub-layers (c) Pre-LN Transformer (d) Post-LN Transformer

Figure 3. The norm of gradients of 1. different layers in the 6-6 Transformer (a,b). 2. $W^{2,L}$ in different size of the Transformer (c,d).

`https://arxiv.org/pdf/2002.04745`

Pre-vs-post Layer normalization (Xiong et al. 20')

The resulting impact on loss and accuracy

Mathematical Institute

Pre-layer-normalization (acts on all of X) shows reduced loss and superior accuracy for translation (BERT), paraphrasing (MRPC), and if sentences are "entangled" (RTE).

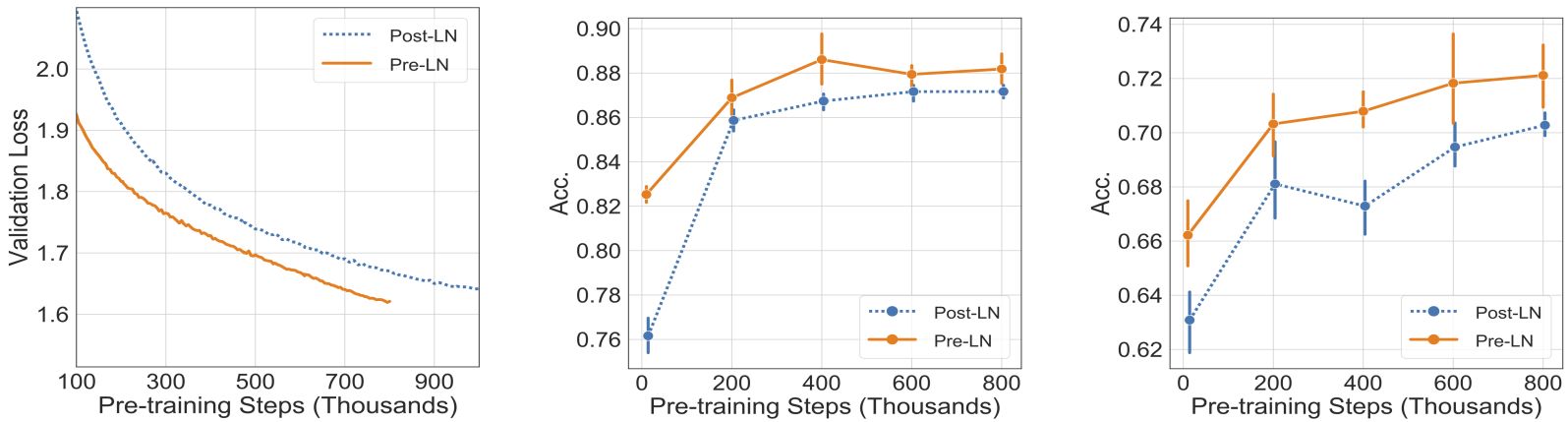

(a) Validation Loss on BERT (b) Accuracy on MRPC (c) Accuracy on RTE

Figure 5. Performances of the models on unsupervised pre-training (BERT) and downstream tasks

`https://arxiv.org/pdf/2002.04745`

Dropout: smoothing the loss landscape

Dropout (Srivastava et al. 14')

Setting hidden layer entries to zero at random

UNIVERSITY OF OXFORD
Mathematical Institute

Dropout is a method by which, during training, the activations are set to zero with some probability. Note, dropout is only used in the training phase, not in testing.

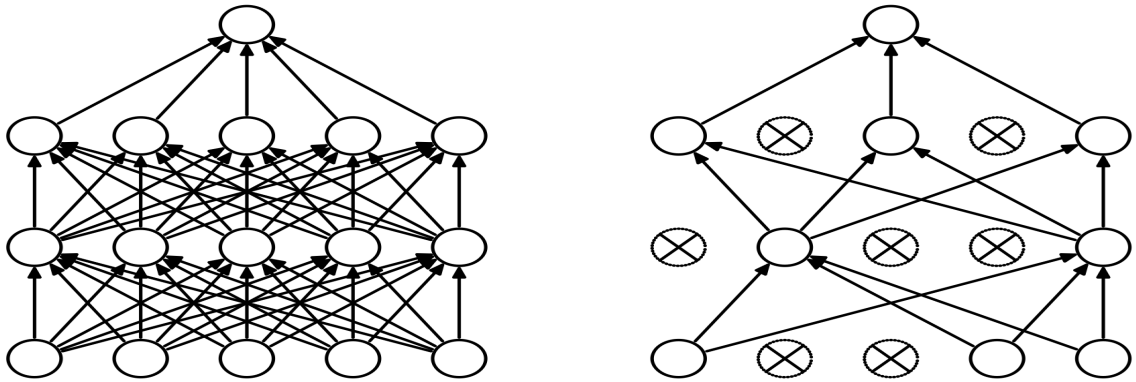

(a) Standard Neural Net (b) After applying dropout.

Figure 1: Dropout Neural Net Model. **Left**: A standard neural net with 2 hidden layers. **Right**: An example of a thinned net produced by applying dropout to the network on the left. Crossed units have been dropped.

Dropout has a number of valuable consequences: reducing correlation in training, inducing sparsity, avoiding overfitting, and can be used to evaluate uncertainty in a deep net.

`http://jmlr.org/papers/volume15/srivastava14a/srivastava14a.pdf`

Dropout (Srivastava et al. 14')

Improved test error

Mathematical Institute

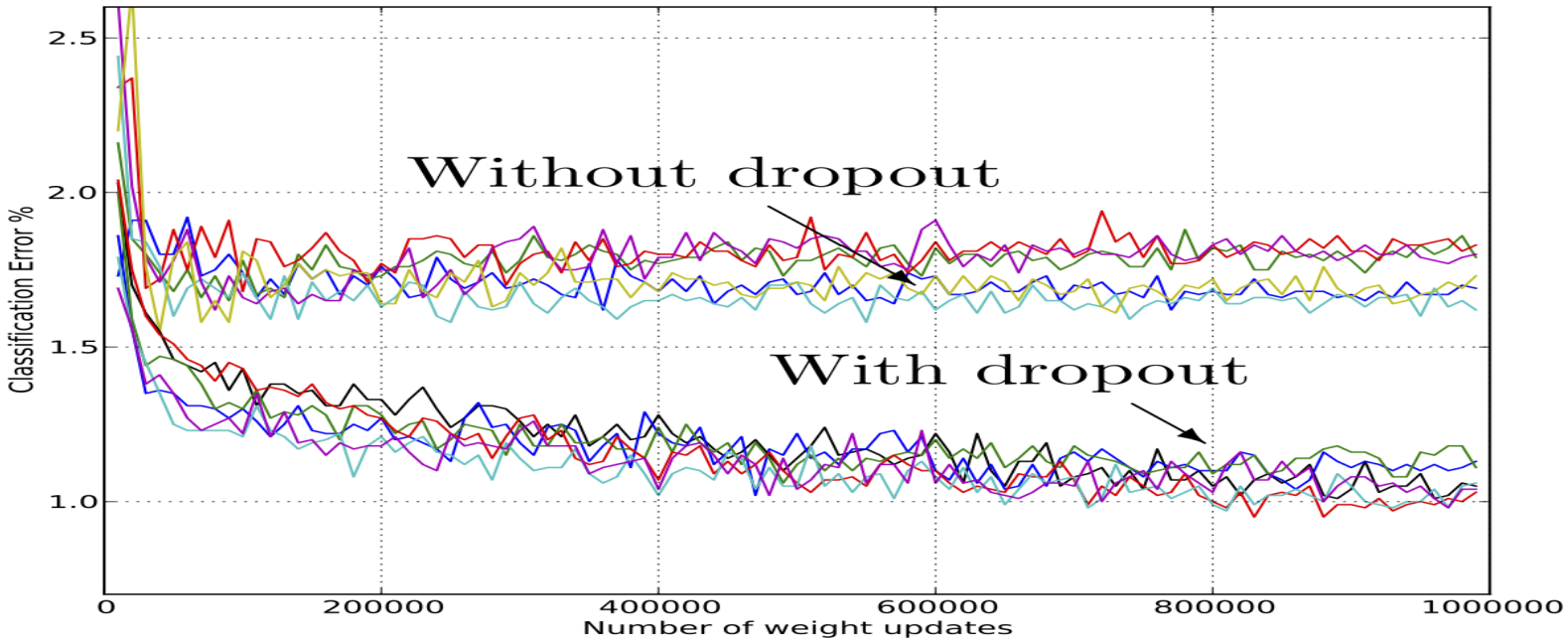

Figure 4: Test error for different architectures with and without dropout. The networks have 2 to 4 hidden layers each with 1024 to 2048 units.

http://jmlr.org/papers/volume15/srivastava14a/srivastava14a.pdf

Dropout less effective for LLMs (Liu et al. 25')

Impact of drop-out is architecture dependent

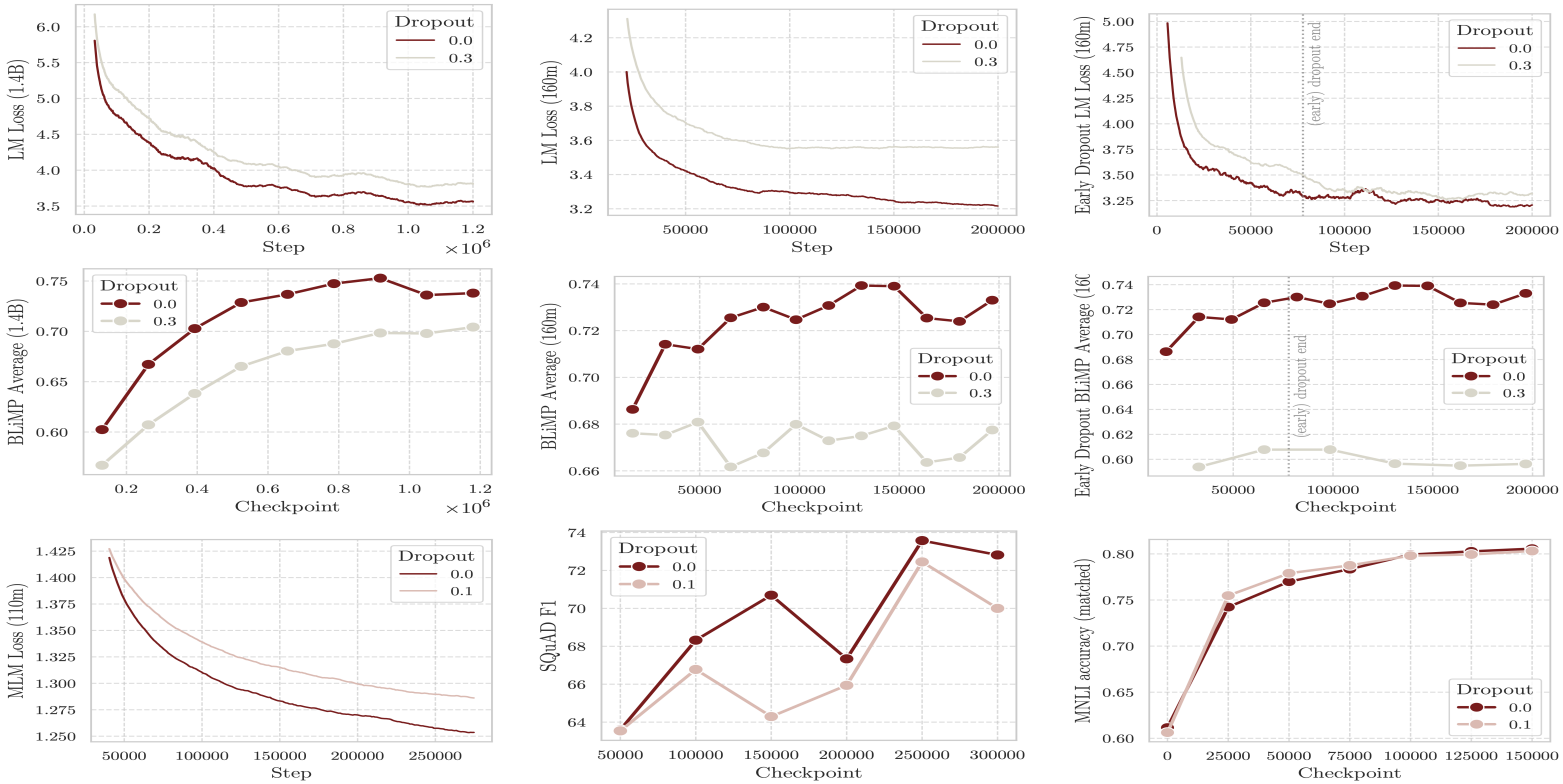

Figure 1: top: language modeling loss with dropout $p = 0.0$, $p = 0.3$, and early dropout for decoder LMs; middle: mean BLiMP scores for these models; bottom: masked language modeling loss with dropout $p = 0.0$, $p = 0.1$, SQuAD F1 (answerable) dev-set scores, and matched MNLI scores.

https://arxiv.org/pdf/2505.24788

Convexification of the network

Convexifying CNN parameters pt. 1 (Zhang et al. 16')

The CNN structure has further non-convexity

Mathematical Institute

Consider a two layer convolutional neural network composed of one convolutional layer followed by a fully connected layer.
Rather than working with x directly, form P vectors $z_p(x)$ for $p = 1, \ldots, P$ where $z_p(x)$ is the portion of x on patch p of the convolutional layer. Then the k^{th} component of $H(x, \theta)$ is given by

$$H(x,\theta)_k = \sum_{j=1}^{r} \sum_{p=1}^{p} \alpha_{k,j,p} \phi(w_j^T z_p(x)).$$

Alternatively if we exclude the nonlinearity we can express this by:

$$\sum_{j=1}^{r} \sum_{p=1}^{p} \alpha_{k,j,p} \phi(w_j^T z_p(x)) = \sum_{j=1}^{r} Z(x) w_j$$

where $Z(x)$ has $z_p(x)$ as its p^{th} row.
`https://arxiv.org/pdf/1609.01000.pdf`

Convexifying CNN parameters pt. 2 (Zhang et al. 16')

Low-rank non-convexity of CNNs

Using the trace formula this can be further condensed to

$$H(x,\theta)_k = \mathrm{tr}\left(Z(x)\left(\sum_{j=1}^{r} w_j \alpha_{k,j}^T\right)\right) = \mathrm{tr}\left(Z(x)A_k\right)$$

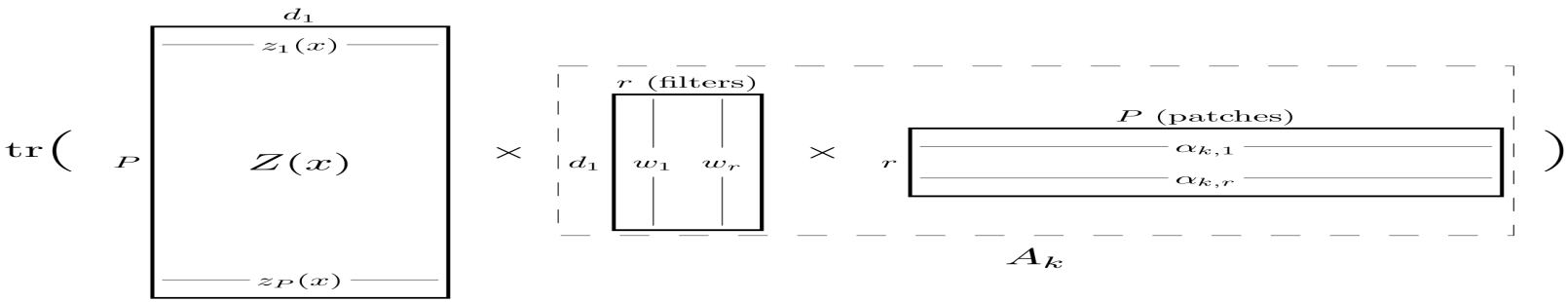

The network parameters are given by A_k nonlinearity is imposed by the A_k having rank r, and we can express all of the parameters of the matrix by A which is similarly rank r.

`https://arxiv.org/pdf/1609.01000.pdf`

Convexifying CNN parameters pt. 3 (Zhang et al. 16')

Convex relaxations are commonly used regularisers

UNIVERSITY OF OXFORD
Mathematical Institute

One can impose the network structure through A, but remove the non-convex rank constraint by replacing a convexification, that is the sum of the singular values of A (Schatten-1, or nuclear, norm).

If the convolutional filters and fully connected rows are uniformly bounded in ℓ^2 by B_1 and B_2 respectively, then one can replace then the sum of the singular values of A are bounded by $B_1 B_2 r\sqrt{n}$ where n is the network output dimension, the network parameters can be considered by varying the nuclear norm bound between 0 and $B_1 B_2 r\sqrt{n}$.

The resulting learning programme is fully convex and can be efficiently solved. The above can be extended to nonlinear activations and multiple layers, learning one layer at a time.
`https://arxiv.org/pdf/1609.01000.pdf`

Convexified CNN: MNIST (Zhang et al. 16')

Improved accuracy for shallow nets

UNIVERSITY OF OXFORD
Mathematical Institute

	basic	rand	rot	img	img+rot
SVM_{rbf} [44]	3.03%	14.58%	**11.11%**	22.61%	55.18%
NN-1 [44]	4.69%	20.04%	18.11%	27.41%	62.16%
CNN-1 (ReLU)	3.37%	9.83%	18.84%	14.23%	45.96%
CCNN-1	**2.38%**	**7.45%**	13.39%	**10.40%**	**42.28%**
TIRBM [38]	-	-	**4.20%**	-	35.50%
SDAE-3 [44]	2.84%	10.30%	9.53%	16.68%	43.76%
ScatNet-2 [8]	1.27%	12.30%	7.48%	18.40%	50.48%
PCANet-2 [9]	**1.06%**	6.19%	7.37%	10.95%	35.48%
CNN-2 (ReLU)	2.11%	5.64%	8.27%	10.17%	32.43%
CNN-2 (Quad)	1.75%	5.30%	8.83%	11.60%	36.90%
CCNN-2	1.38%	**4.32%**	6.98%	**7.46%**	**30.23%**

Table 1: Classification error on the basic MNIST and its four variations. The best performance within each block is bolded. The tag "ReLU" and "Quad" means ReLU activation and quadratic activation, respectively.

`https://arxiv.org/pdf/1609.01000.pdf`

Convexified CNN: CIFAR10 (Zhang et al. 16')

Monotonically decreasing training objective

	Error rate
CNN-1	34.14%
CCNN-1	**23.62%**
CNN-2	24.98%
CCNN-2	**20.52%**
$\text{SVM}_{\text{Fastfood}}$ [27]	36.90%
PCANet-2 [9]	22.86%
CKN [30]	21.70%
CNN-3	21.48%
CCNN-3	**19.56%**

Table 3: Classification error on the CIFAR-10 dataset. The best performance within each block is bolded.

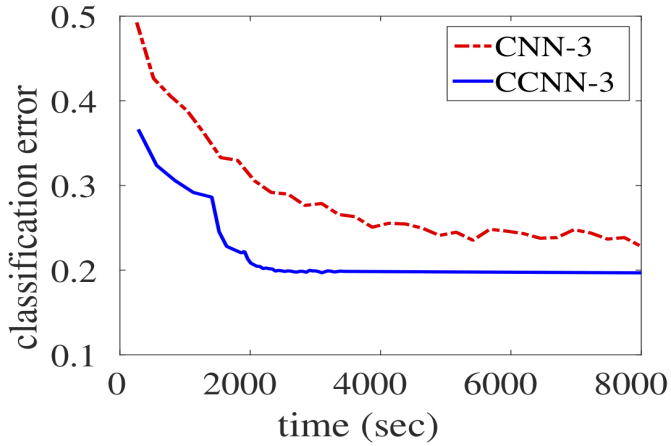

Figure 4: The convergence of CNN-3 and CCNN-3 on the CIFAR-10 dataset.

	CNN-1	CNN-2	CNN-3
Original	34.14%	24.98%	21.48%
Convexified	**23.62%**	**21.88%**	**18.18%**

Table 4: Comparing the original CNN and the one whose top convolution layer is convexified by CCNN. The classification errors are reported on CIFAR-10.

`https://arxiv.org/pdf/1609.01000.pdf`

Improving the loss landscape summary

Influence of network architecture and training choices

Mathematical Institute

- Larger training batch size narrows the loss function while weight decay (adding $\|\theta\|$ to the loss, broadens the loss function.
- Adding skip connections through residual networks can greatly smooth the loss landscape.
- Batch normalization can help train parameters in bulk and in so doing improve the training rate; though superfluous for expressivity.
- CNNs can even be convexified which may limit overall accuracy, but ensures ease of training regardless of initialization.